Low-Noise Block Downconverter based on COTS and SIW Filters for Ku-band Cubesat Transponders

Giulia Orecchini
Dept. of Engineering
University of Perugia
Perugia, Italy
giulia.orecchini@unipg.it

Giacomo Schiavolini
Dept. of Engineering
University of Perugia
Perugia, Italy
giacomo.schiavolini@studenti.unipg.it

Paolo Mezzanotte
Dept. of Engineering
University of Perugia
Perugia, Italy
paolo.mezzanotte@unipg.it

Simone Pauletto
PICOSATS s.r.l.
Area Science Park
Trieste, Italy
simonepauletto@picosats.eu

Andrea Loppi
PICOSATS s.r.l.
Area Science Park
Trieste, Italy
andrealoppi@picosats.eu

Andrea Beltramello
PICOSATS s.r.l.
Area Science Park
Trieste, Italy
andreabeltramello@picosats.eu

Federico Dogo
PICOSATS s.r.l.
Area Science Park
Trieste, Italy
federicodogo@picosats.eu

Davide Manià
PICOSATS s.r.l.
Area Science Park
Trieste, Italy
davidemania@picosats.eu

Valentina Palazzi
Dept. of Engineering
University of Perugia
Perugia, Italy
valentina.palazzi@unipg.it

Guendalina Simoncini
Dept. of Engineering
University of Perugia
Perugia, Italy
guendalina.simoncini@studenti.unipg.it

Luca Roselli
Dept. of Engineering
University of Perugia
Perugia, Italy
luca.roselli@unipg.it

Anna Gregprio
Dept. of Physics
University of Trieste
Trieste, Italy
anna@picosats.eu

Mario Fragiacomo
PICOSATS s.r.l.
Area Science Park
Trieste, Italy
mario@picosats.eu

Federico Alimenti
Dept. of Engineering
University of Perugia
Perugia, Italy
federico.alimenti@unipg.it

***Abstract*—This paper proposes a Low-Noise Block (LNB) downconverter operating in the Ku-band for Cubesat transponders. The frontend is composed by a Low-Noise Amplifier (LNA) and two switchable Substrate Integrated Waveguide (SIW) filters, providing a frequency reconfigurability to the system. The LNB is completed by a downconversion unit, constituted by a mixer, a PLL frequency synthesizer and an IF amplifier. A first breadboard features an overall gain of 54 dB with a 2.3 dB noise figure. The worst case linearity performance indicates an input-referred 1 dB compression point (P1dB) and a third-order intercept point (IIP3) equal to -27 dBm and -16 dBm respectively. This work is important since demonstrates a low-cost solution for satellite radio apparatuses based on commercial components and standard PCB.**

***Index Terms*—Cubesats, low-noise block, RF/microwave electronics, Ku-band transponders.**

I. Introduction

Cubesats are miniaturized platforms with a great potential for science, telecommunication and, more in general, for future space-based services like the Internet of Space (IoS), [1]. In the IoS scenario, Cubesats not only plays the role of network infrastructure bringing the Internet to remote places, but provide connecting capabilities to sensors that, in principle, can be located everywhere in the world [2], [3]. Their usage helps also in reducing space debris, since Cubesats can be deorbited easily [4].

The increasing Cubesat market requests high-performance and low-cost satellite radios and antennas [5]. The classical approach is based on hybrid modules placed into a metal housing with cavities shielding the different receiver stages [6], [7]. Even though such a construction gives high flexibility in terms of interfaces and during the characterization phase, it results to be bulky and is not feasible for the proposed applications. On the other hand shieldless solutions have already been proposed, but the developed receivers use a single filter [8].

In this paper we present, for the first time, a Ku-band LNB downconverter that features a frequency reconfigurability in two sub-bands, namely the 13-GHz and the 14-GHz uplink sub-bands allocated for GEO satellite services. The developed system is based on Components Off The Shelf (COTS) and uses two switchable image-reject filters implemented in Substrate Integrated Waveguide (SIW) technology. The SIW filters are self-shielded devices: in this way the receiver can be completely integrated into a commercial Printed Circuit Board (PCB), and complex mechanical designs with shielding cavities are avoided. This design approach is experimentally validated, opening the way to a novel generation of low-cost satellite radios and radiometers [9].

II. System overview

The proposed system is a transponder operating in the GEO stationary Ku frequency band. An uplink signal between 12.75 to 14.80 GHz is received, amplified, filtered, frequency converted and transmitted back to Earth. The downlink signal is between 10.70 to 12.75 GHz. The block diagram of the transponder is shown in Fig. 1. No demodulation, error correction and modulation functions are present in the system so that the transponder is said to be "transparent".

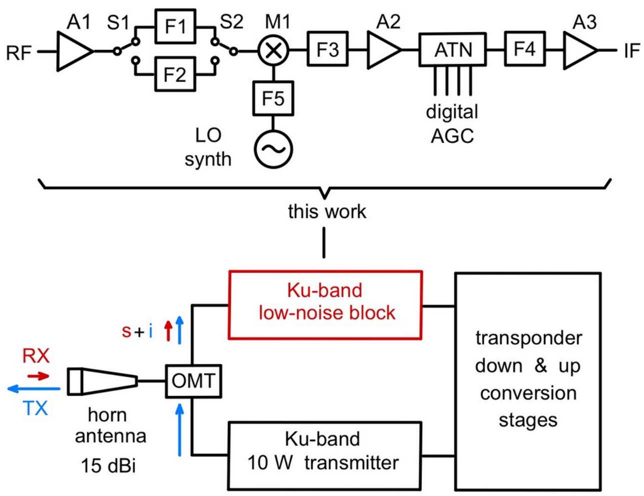

Fig. 1. Simplified block diagram of the Ku-band LNB downconverter. The system operates in full-duplex mode, simultaneously transmitting and receiving signals with a single horn antenna in orthogonal polarization.

Such an apparatus works in full-duplex mode, simultaneously transmitting and receiving signals with the same horn antenna. An Ortho-Mode Transducer (OMT) separates TX and RX signals, providing an isolation of about 70 dB. Since a 10 W (40 dBm) transmitter is used, a -30 dBm self interference is generated: a power level that is several order of magnitude greater than the -100 dBm signal expected from the ground station. This poses serious linearity problems to the receiver. In particular, because uplink and downlink frequency bands overlap, a frontend with switchable image-reject filters in Substrate Integrated Waveguide (SIW) technology is adopted (see A1, F1, F2, S1 and S2 in the figure).

The LNB downconverter chain is completed by a mixer (M1), a Local Oscillator (LO) based on a Phase-Locked Loop (PLL) synthesizer, and an Intermediate Frequency (IF) amplifier (A2, A3, F3, F4) operating at 2185 MHz. A digitally controlled attenuator (ATN) is used to implement the Automatic Gain Control (AGC).

III. Materials and methods

In order to keep low the LNB cost, a commercial PCB technology is adopted. The PCB stackup is composed by 4-layers, with the top and bottom ones made out of RO4350B material (thickness $254\,\mu$m, $\epsilon_r = 3.48$, $\tan\delta = 0.004$), and the two internal ones implemented with FR4 (thickness $508\,\mu$m including prepreg, $\epsilon_r = 4.6$, $\tan\delta = 0.02$). With the chosen fabrication process it is possible to realize a minimum track width and a spacing of 0.15 mm, a minimum via diameter of 0.2 mm and to implement buried via interconnections.

As previously illustrated, a frontend with switchable image-reject filter is adopted because TX (downlink) and RX (uplink) bands overlap. The uplink frequency range is so divided into two sub-bands, namely: the 13-GHz sub-band from 12.75 to 13.25 GHz and the 14-GHz sub-band from 13.75 to 14.8 GHz. The filters F1 and F2 are implemented in SIW technology according to [10], because the obtained devices are self shielded and fully integrated in the PCB. F1 and F2 are constituted by four resonant cavities coupled with inductive irises, and include input/output Grounded Co-Planar Waveguide (GCPW) to SIW transitions. The design method is based on the approach suggested, in 2008, by Wu *et al.* [11], and makes extensive use of 3D electromagnetic simulations [12].

Apart for the SIW filters, all the other elements are COTS already available on the market. The LNA features a 27 dB power gain and a 1.4 dB noise figure. Its linearity (-15 dBm input 1 dB compression point) is enough to tolerate the -30 dBm self interference without saturation. The two solid-state SPDT switches have an insertion loss of 2.2 dB and an isolation of 40 dB. The mixer has a 8 dB conversion loss when driven by a 13 dBm oscillator (an amplifier is used in the LO chain). The IF filters shows a typical insertion loss of 2 dB and a -3 dB bandwidth of 55 MHz. A2 and A3 are high-linearity 20 dB gain blocks, whereas a 7-bit variable attenuator with 0.25 dB steps (ATN) is used for the AGC.

IV. Results

The switchable SIW filter configuration is validated with the test PCB shown in Fig. 2 (top panel), that includes S1, S2, F1 and F2 of the block diagram. The scattering parameters of the board have then been measured with a Vector Network Analyzer (VNA) and are reported in the two bottom panels. Simulations agree well with measurements, unless for an underestimation of the insertion losses, due to substrate material tolerances, coaxial adapters and routing miscrostrip lines (not considered in the model). The center frequency insertion losses are: 10.2 dB measured against 7.2 dB simulated (13 GHz filter selected by switches); 8.5 dB measured against 5.9 dB simulated (14 GHz filter selected by switches).

A LNB downconverter breadboard is then implemented as illustrated in Fig. 3. To facilitate the system debug, each element of the block diagram is realized with separate PCBs that are then connected by coaxial adapters. To perform linearity tests in the worst case, and to assess the self-interference immunity, the switchable filters have not been taken into consideration during the first experiment. In the proposed configuration the LNB power consumption is of about 3.2 W including the LO signal generation chain.

The linearity is evaluated with both single and two tones tests. The LNB downconverter compression point (single tone measurement) is equal to about -27 dBm (ATN set for max

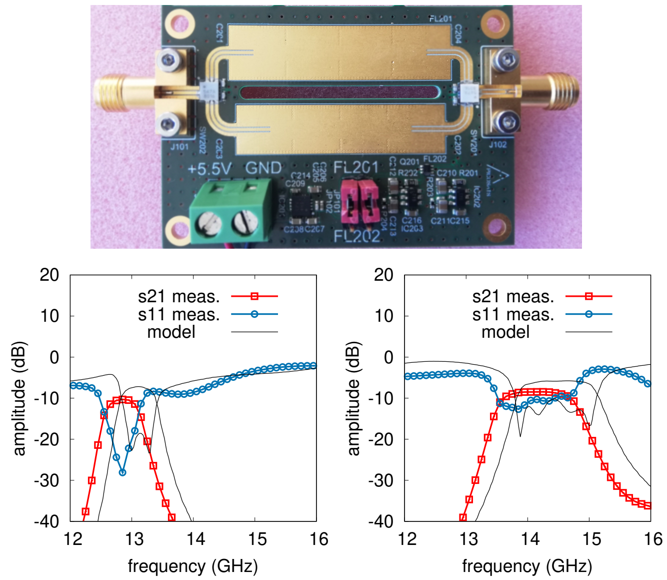

Fig. 2. Fabricated test PCB with switchable SIW filters (top) and comparison between measured and simulated scattering parameters (bottom). 13 GHz filter-switch response (left); 14 GHz filter-switch response (right).

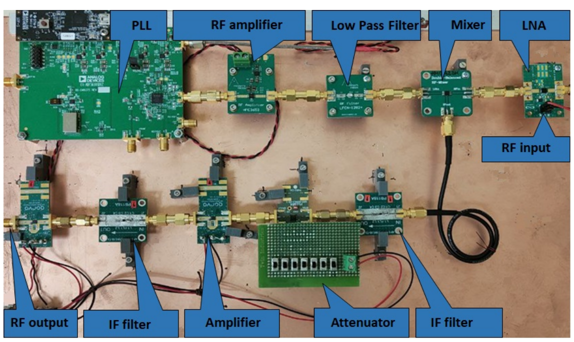

Fig. 3. Breadboard of the Ku-band low-noise downconverter. This implementation is without switchable image-rejection SIW filters in order to carry out linearity experiments in the worst conditions.

gain), and remains almost constant in the considered frequency band. Fig. 4 reports the results of a test with two tones that, once downconverted, fall within the IF filter bandwidth. In particular, the tone frequencies are: $f_1 = 12775\,\text{MHz}$ and $f_2 = 12805\,\text{MHz}$ (with a $30\,\text{MHz}$ spacing). The local oscillator is set to $10605\,\text{MHz}$, and each tone has an available power level of $-43\,\text{dBm}$ at the receiver input. In this condition the output fundamentals are at $0\,\text{dBm}$, whereas the in-band third-order intermodulation products (IM3) are equal to $-54\,\text{dBm}$. Applying well known relationships we get an input-referred third-order intercept point (IIP3) of $-16\,\text{dBm}$. In a second experiment the receiver is tuned on a certain channel and two interferences at the lower adjacent channels are injected at its input (see Fig. 5). The tone frequencies are: $f_1 = 12690\,\text{MHz}$ and $f_2 = 12740\,\text{MHz}$, with a $50\,\text{MHz}$ channel step. The local oscillator is set to $10605\,\text{MHz}$, in such a way as to receive a signal at $2\,f_2 - f_1 = 12790\,\text{MHz}$, i.e. the higher third-order intermodulation product between f_1 and f_2. This signal

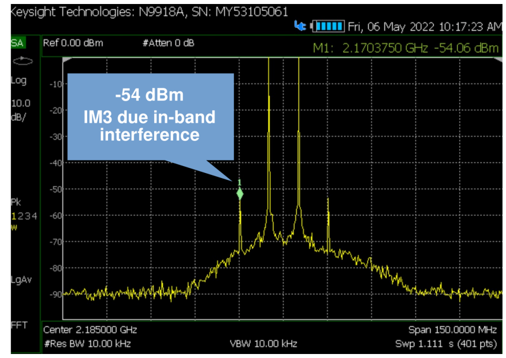

Fig. 4. Third-order intermodulation experiment with two $-43\,\text{dBm}$ tones falling in the IF filter bandwidth. This test is useful to determine the system IIP3. LNB gain set to 43 dB by the variable attenuator.

doesn't exist at the input, but is generated by the LNA/mixer non linearities, and is present at IF with a level of $-77.4\,\text{dBm}$ (slightly above to the receiver noise floor). The input power level of the two tones is $-45\,\text{dBm}$ and, although attenuated by the IF filter, they are still visible in the output spectrum. The obtained, worst-case linearity performance are quite good and validate the system design.

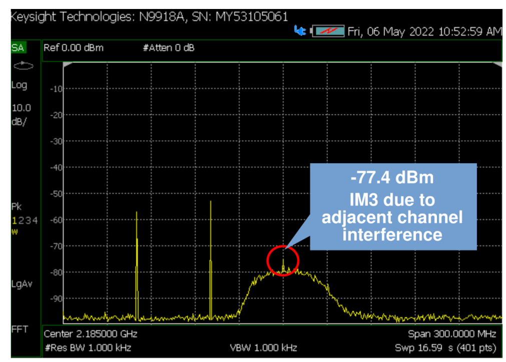

Fig. 5. Third-order intermodulation experiment with the LNB downconverter tuned on a certain channel and two $-45\,\text{dBm}$ interferences at the lower adjacent channels. This test is useful to asses the interference robustness of the system. LNB gain set to 43 dB by the variable attenuator.

Finally noise measurements have been carried out on the developed board, as shown in Fig. 6. In this experiment the LO is fixed at 11815 MHz (14-GHz channel) and a HP346C-K01 laboratory noise source is applied to the LNB input. The 14-GHz SIW filter is inserted between LNA and mixer to reject the image frequency noise components. A HP8970 noise figure test set is used to measure system gain (red line) and noise figure (blu line). The obtained LNB downconverter performance are: 54 dB gain (ATN set for max gain) and 2.3 dB noise figure. The gain agrees well with that modeled using the building-block data sheets values (black point in the figure).

V. Conclusions

This work demonstrates that LNB downconverters based on COTS are feasible at low-cost and can operate in the Ku-band allocated for space services. A frontend configuration

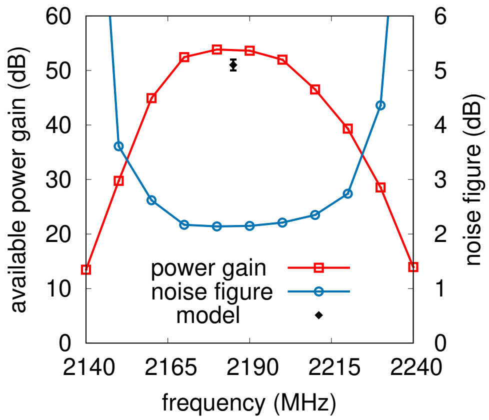

Fig. 6. Measured available power gain and noise figure of the whole LNB downconverter in the IF band. Comparison with data sheet estimations.

with LNA and switchable SIW filters is demonstrated for the first time. A breadboard without filters is then used to asses the LNB linearity in the worst case. The obtained results shows that the system can safely tolerate the -30 dBm self interference produced by the 10 W transmitter. Finally, all the considered circuits can be sufficiently miniaturized to stay in a Cubesat, are compatible with commercial PCB technology and doesn't require complex shielding mechanics.

ACKNOWLEDGEMENTS

This work was supported in part by the the Italian Ministry of University and Research (MUR), in the frame of the "PON 2022 Ricerca e Innovazione" action.

REFERENCES

[1] *Achieving Science with CubeSats: Thinking Inside the Box*, The National Academies Press, Washington, DC, USA, 2016. [Online]. Available: https://www.nap.edu/catalog/23503/achieving-science-with-cubesats-thinking-inside-the-box
[2] M. Harris, "Tech giants race to build orbital internet," *IEEE Spectrum*, vol. 55, no. 6, pp. 10–11, Jun. 2018.
[3] M. Mitry, "Routers in space: Kepler communications' CubeSats will create an Internet for other satellites," *IEEE Spectrum*, vol. 57, no. 2, pp. 38–43, Feb. 2020.
[4] J. Hsu, "Fishing for space junk," *IEEE Spectrum*, vol. 55, no. 6, pp. 7–9, Jun. 2018.
[5] N. Chahat, "A mighty antenna from a tiny cubesat grows," *IEEE Spectrum*, vol. 55, no. 2, pp. 32–37, Feb. 2018.
[6] M. Comparini, M. Feudale, J. Linkowski, P. Ranieri, and A. Suriani, "Fully integrated Ka/K band hermetic receiver module," in *30th European Microwave Conference*, Paris (F), Oct. 2000.
[7] D. Roy, A. Choudhury, M. Mohiyuddin, A. Sucharitha, and D. Ramana, "Design and realisation of ku-band tele-command and ranging receiver for satellite application," in *IEEE MTT-S International Microwave and RF Conference (IMaRC)*, Kolkata, India, Nov. 2018, pp. 1–4.
[8] F. Alimenti, P. Mezzanotte, G. Simoncini, V. Palazzi, R. Salvati, G. Cicioni, L. Roselli, F. Dogo, S. Pauletto, M. Fragiacomo, and A. Gregorio, "A ka-band receiver front-end with noise injection calibration circuit for cubesats inter-satellite links," *IEEE Access*, vol. 8, pp. 106 785–106 798, Jun. 2020.
[9] F. Berrilli, A. Bigazzi, L. Roselli, P. Sabatini, M. Velli, F. Alimenti, F. Cavallini, V. Greco, P. Moretti, S. Orsini, M. Romoli, S. White, and the ADAHELI Team, "The ADAHELI solar mission: Investigating the structure of the sun's lower atmosphere," *Advances in Space Research*, vol. 45, no. 10, p. 1191–1202, May 2010.
[10] F. Alimenti, P. Mezzanotte, V. Palazzi, L. Roselli, F. Dogo, and M. Fragiacomo, "Microwave receiver device," European Patent 21 169 960.8, Apr. 21, 2021.
[11] X.-P. Chen and K. Wu, "Substrate integrated waveguide cross-coupled filter with negative coupling structure," *IEEE Trans. on Microwave Theory and Techniques*, vol. 56, no. 1, pp. 142–149, Jan. 2008.
[12] F. Alimenti, P. Mezzanotte, L. Roselli, and R. Sorrentino, "Efficient analysis of waveguide components by FDTD combined with time domain modal expansion," *IEEE Microwave Guided Wave Letters*, vol. 5, no. 10, pp. 351–353, Oct. 1995.